Soft Matter

Accepted Manuscript

ROYAL SOCIETY OF CHEMISTRY

www.rsc.org/softmatter

Journal Name

ARTICLE TYPE

Cite this: DOI: 10.1039/xxxxxxxxxx

A robust and reproducible procedure for cross-linking thermoset polymers using molecular simulation†

Baris Demir[a] and Tiffany R. Walsh*[a]

Received Date
Accepted Date

DOI: 10.1039/xxxxxxxxxx

www.rsc.org/journalname

Molecular simulation can provide valuable guidance in establishing clear links between structure and function to enable the design of new polymer-based materials. However, molecular simulation of thermoset polymers in particular, such as epoxies, present specific challenges, chiefly in the credible preparation of polymerised samples. Despite this need, a comprehensive, reproducible and robust process for accomplishing this using molecular simulation is still lacking. Here, we introduce a clear and reproducible cross-linking protocol to reliably generate three dimensional epoxy cross-linked polymer structures for use in molecular simulations. This protocol is sufficiently detailed to allow complete reproduction of our results, and is applicable to any general thermoset polymer. Amongst our developments, key features include a reproducible procedure for calculation of partial atomic charges, a reliable process for generating and validating an equilibrated liquid precursor mixture, and establishment of a novel, robust and reproducible protocol for generating the three-dimensional cross-linked solid polymer. We use these structures as input to subsequent molecular dynamics simulations to calculate a range thermo-mechanical properties, which compare favourably with experimental data. Our general protocol provides a benchmark for the process of simulating epoxy polymers, and can be readily translated to prepare and model epoxy samples that are dynamically cross-linked in the presence of surfaces and nanostructures.

Epoxy polymers have been widely used in various industries due to their excellent thermal and mechanical properties, resistance to corrosion, with a high strength[1] and low shrinkage[2]. Their capability of adhesion to various substrates and chemical compatibility make epoxies appropriate candidates for composite materials. In the solid phase epoxy polymers comprise a three-dimensional (3-D) cross-linked polymer network, where C–N cross-link bonds exist between the polymer repeat unit (which typically contains epoxide groups) and the hardening agent (which typically contains amine groups). The degree of cross-linking is defined as the ratio between the number of reacted epoxy carbon atoms and the total number of epoxy carbon atoms in the system. For epoxy polymers based on EPON and DETDA, or similar precursors, the degree of cross-linking has a substantial effect on the resulting thermo-mechanical properties, typically with the material increasing in rigidity and stiffness with an increase in cross-linking degree.

The principal benefit of applying molecular dynamics (MD) simulation to the study of epoxy polymers lies in the ability to forge immediate connections between the molecular-scale structure of the material and its physical, chemical and mechanical properties. However, these outcomes are strongly reliant on the process used to generate the complex, amorphous 3-D polymer structures inherent to these systems. Central to this is a robust computational process for the *in-situ* creation of cross-link bonds. While numerous approaches to generating and modelling these epoxy polymer networks have been previously published, these published protocols all suffer from either a lack of reported methodological detail, which prevents reproducability, and/or are based on inappropriately small systems or short simulation timescales, and/or have not demonstrated sufficient statistical sampling. The lack of reproducability in this area hinders debate and therefore slows the advancement of this field.

Numerous previous studies focusing on the molecular modeling of epoxy polymer materials have been published in the literature[3–25]. Also, cross-linking modelling is being studied in other fields[26]. In the following overview we will mention only those works in which the development of a dynamic cross-linking

[a] *Institute for Frontier Materials, Deakin University, Geelong, Australia. Fax: +61 (0)3 5227 1103; Tel: +61 (0)3 5227 3116; E-mail: tiffany.walsh@deakin.edu.au*

† Electronic Supplementary Information (ESI) available: additional methodological details, atomic parameters for charge calculations, ideal bond lengths and force constants for the relaxation protocol, calculated partial atomic charges, labels for unique atomic environments in each molecule, molecular structure of the secondary amine reaction, reference sites for the radial distribution functions, schematic of the 0.2% offset convention, pure liquid densities, liquid mixture densities, evolution of the liquid mixture structure with time, bond lengths and angles in the polymerised samples, pressure of the polymerised samples, Young's modulus data, and yield strength and yield strain calculated via the 0.2% offset line. See DOI: 10.1039/b000000x/

methodology was reported [9,10,19]. All of the approaches discussed herein are based on identifying candidate atom pairs for cross-linking, based on spatial criteria, chiefly cut-off distances between relevant atom pairs. Our approach makes use of all-atom MD simulations. We note that one of the earliest multi-scale approaches was reported by Komarov *et al.* [7], who made use of coarse-graining partnered with Monte Carlo simulations to cross-link their samples, and reverse-mapping partnered with MD simulations of the resulting cross-linked network. Further details on computer modelling of thermoset resins in general can be found in the excellent review by Li and Strachan [27].

Some early approaches to modelling cross-linked epoxy polymers were based on the construction of a free-standing (*i.e.* non-periodic) dendrimer-like structures, [4,8,28]. Such an approximation is inherently limiting, since it cannot be used to generate credible samples of epoxy polymerized *in situ* in the presence of surfaces or nanostructures. Nonetheless, the work of Bandyopadhyay and Odegard [15] warrants discussion. In this work the authors generated small dendrimers and then cross-linked these in larger arrays, in order to capture the impact of cross-link inhomogeneity on the properties of their polymer samples. However, the outcomes from these studies were not conclusive, which might be attributed to the small dendrimer sizes considered in this work. The spirit of this approach might warrant further refinement in addition with implementation on longer length-scales.

In contrast to the 'dendrimer' static approach, Varshney *et al.* [9] reported the development of a dynamic epoxy cross-linking procedure for atomistic simulations, where a spatial cutoff criterion was used. These authors first generated a liquid mixture sample and subjected this to a very short MD simulation. As we shall indicate herein, this protocol does not guarantee satisfactory equilibration of the liquid mixture structure. After this equilibration step, these authors applied a cross-linking procedure that involved a variable cut-off distance ranging from 4–10 Å, along with a brief constant pressure MD simulation (in the isothermal-isobaric *NPT* ensemble) after each set of cross-link bonds were formed.

In a more recent study, Li and Strachan [10] modelled the cross-linking reaction between EPON-862 and DETDA molecules via a multi-step relaxation approach. For their cross-linking process, these authors used a fixed cut-off distance (pre-defined as 4 $\times$ the equilibrium bond distance for the cross-link bond). After each round of cross-link bond formation, they applied a multi-step geometry optimisation (not MD simulation) process, in which the ideal cross-link (C–N) bond length and ideal cross-link bond force constant were gradually decreased and increased respectively, to relax the internal stress. Moreover, as for many other previously-published simulation studies in this field, the simulation details provided were not sufficient to permit full reproduction of these results. This was also the case for the partial atomic charge calculation reported in this study. Recently, Khare and Khare [17] reported the use of a similar multi-step relaxation procedure, but these authors instead used MD simulation during their step-wise relaxation process. However, these authors also used a single (long) cutoff distance to identify relevant atom pairs.

In a further variation on these procedures, Odegard *et al.* [19] used a combination of force-fields in their study of the EPON-862/DETDA system. These authors used the OPLS [29] force-field to manually generate the 3-D cross-linked structure, but then, somewhat counter-intuitively, switched to the reactive force-field (ReaxFF) [30] *after* formation of the cross-link bonds, to calculate the thermo-mechanical properties of the resulting 3-D samples. These authors justified this choice based on the current immaturity of ReaxFF as regards the dynamic formation of epoxy cross-link bonds. In contrast to many (but not all) cross-linking simulation studies, these authors used several independently-created samples to generate adequate statistical sampling of the resulting thermo-mechanical properties. However, these authors used a fixed cut-off distance and used only geometry optimisation to relax their structures after the formation of the cross-link bonds.

In a related study, Izumi *et al.* [16] modelled the cross-linking of phenolic resins. First, these authors fitted their partial atomic charges for use with the DREIDING force-field from the results of density functional theory calculations. Next, these authors then subjected their precursor liquid mixture sample to brief MD simulation. During this simulation the authors saved twenty different near-successive snapshots (every 10 ps) of the trajectory. Therefore, while these authors produced twenty different samples for subsequent cross-linking, by definition their process did not yield independently-generated samples because each of the initial structures would be strongly correlated with the other structures. These authors did not relax their samples as the cross-linking proceeded, but relaxed the structure at the end of the cross-linking process.

Very recently, Masoumi *et al.* [31] reported simulations of the thermo-mechanical properties of the DGEBA-JEFFAMINE D-230 epoxy system. These authors subjected their precursor liquid mixture to thermal (simulated) annealing. However, they did not report any evidence regarding the evolution of the liquid mixture structure as a function of annealing cycle. During the cross-linking process, the sample was relaxed via MD simulation (and annealling), but was not done using multi-step approaches as outlined above. The authors used a variable cut-off distance (up to 14 Å). However, their findings were reported only for a very small system size (48:24 for DGEBA:D-230), which inherently limits the cell simulation size to small values, which could impart detrimental artefacts due to the artificially-small periodicity of the system.

The use of the DREIDING force-field also requires that partial atomic charges for all molecules be generated. Previous studies [10,32–35] that have reported the generation of DREIDING partial atomic charges for epoxy and hardener molecules have lacked unambiguous methodological details for key steps of this process. Given the central importance of the partial atomic charges in determining the properties of materials in these DREIDING simulations, this limitation presents a substantial obstacle to reproducing the results of these previously published studies.

As these examples given above clearly illustrate, none have been shown to fully address all of the limitations and/or inconsistencies that prevent the generation of reproducible and reliable 3-D cross-linked epoxy polymer samples that are demonstrated to be free from internal stress. These limitations and challenges are detailed as follows. First, a clear and reproducible protocol

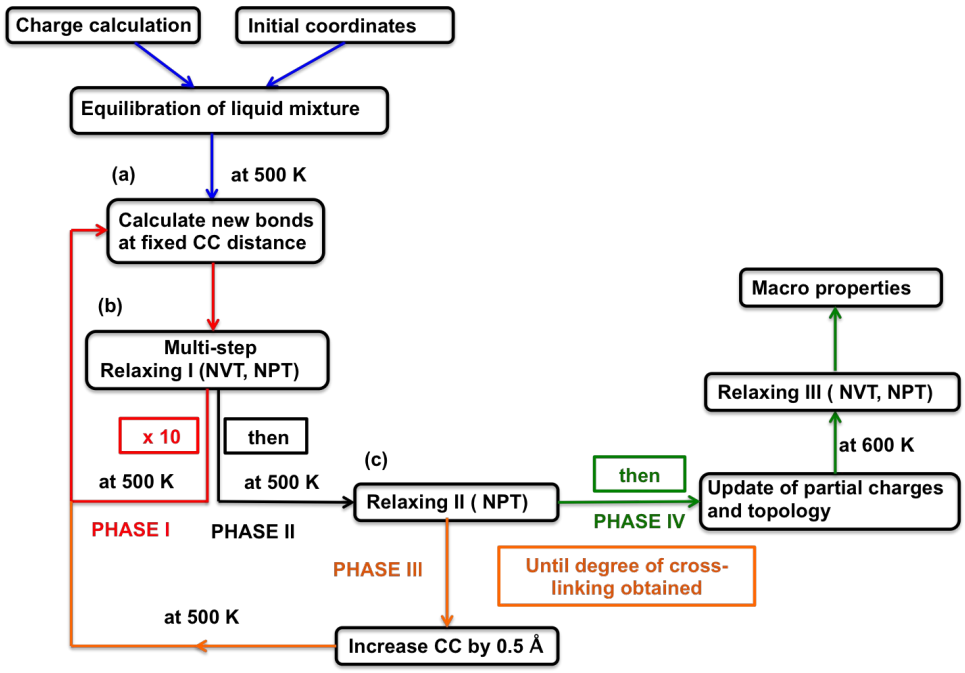

Fig. 1 Summary of our process to generate 3-D cross-linked epoxy polymer samples.

is required for the generation of partial atomic charges for the precursor molecules. The generation of atomic partial charges is not a well-defined problem, and does not admit a unique solution. Therefore, this demand can potentially introduce ambiguity and a lack of reproducibility in the subsequent simulations, if the details of the process used to generate these charges are not carefully reported.

Second, a robust process for obtaining and establishing an equilibrated liquid precursor sample is absolutely necessary. Because the liquid precursor mixture is viscous (from a molecular simulation perspective), care must be taken to ensure the structure of the liquid does not become trapped in metastable configurations. This does not appear to have been demonstrated in most previous reports of epoxy cross-linking simulations. Moreover, we can find no such simulation study that has provided evidence of liquid equilibration prior to cross-linking.

Third, the cross-linking procedure must be clearly defined. Also, in contrast with previously reported studies, the use of variable cut-off distances, along with multi-step relaxation coupled with MD simulation, is required to produce solid polymer structures that are not internally stressed. It is this cross-linking approach that we introduce herein. Fourth, the use of simulation sample replicates is essential. Very few previous studies reported simulation results for more than one independently-generated structural sample (for the same set of cross-linking conditions). One notable exception is the study reported by Shenogina *et al.* [14], who used seventy topologically-distinct structural epoxy models. As our results will demonstrate, use of replicates is essential to capturing average behaviours of the epoxy material. Fifth, careful cooling of the resulting cross-linked sample to room temperature is a key step. Reproducible methodological details for this cooling process must be provided. Finally, substantial system sizes must be considered. Small system sizes inherently limit the size of the simulation cell, making the cell dimensions almost comparable with the long axis of the longest precursor molecule. This therefore potentially imposes artificial periodicity on the system which may lead to misleading results.

In contrast to the limitations and challenges detailed above, here, we describe and detail a robust and systematic development of all such key aspects of cross-linked epoxy polymer modelling, with sufficient detail to ensure all stages can be reproduced by others. To accomplish this, we made use of open-source software for molecular dynamics (MD) simulations. We applied our comprehensive procedure to the generation of 3-D cross-linked samples of the EPON-862/DETDA epoxy system, and used these to calculate thermo-mechanical properties of the polymer, including the glass transition temperature, Young's modulus, Poisson's ratio, and the yield strength and yield strain. All of these quantities were compared with values available from the literature. In addition to being entirely reproducible by others, our cross-linking procedure contains novel features, chiefly a combination that incorporates variation of cross-linking reaction distance in partnership with a multi-step relaxation via MD simulation, that has not been reported before for epoxy polymers. Furthermore, the careful equilibration of the liquid precursor mixture, prior to initiation of the cross-linking process, is comprehensively demonstrated for the first time.

Methods

A schematic of our protocol is illustrated in a flowchart (Figure 1), showing each step of the process. Based on the clarity and reliability of the procedure, our work represents the first reported study in which the reported data can be readily reproduced by following each detailed step. Following a set-up stage, there are four

subsequent phases (see Figure 1) in this protocol. None of these steps required exceptional computational resources to realise.

Basic Simulation Details

All atoms were modelled explicitly using the DREIDING FF[36]. Temperature and pressure were controlled via Nosé-Hoover thermostat[37,38] and barostat[37,39], respectively. The cut-off distance for long range contributions to the potential energy was set to 12 Å. The contribution of long-range interactions to the pressure and energy (beyond the interaction cut-off distance) were calculated via a tail correction and the particle-particle-particle-mesh[40] algorithm. Newton's equations of motion were integrated using a 1 fs time-step throughout all simulations. Periodic boundary conditions were implemented in all three dimensions. The simulations were carried out using the LAMMPS[41] software package (lammps.sandia.gov).

Partial Atomic Charge Calculation

In terms of molecular modelling, partial atomic charges (as distributed over atomic sites) play a crucial role in determining the properties of materials. In our simulations, we have used the DREIDING FF[36], which does not contain partial atomic charges by default; therefore these charges must be calculated. In practice, there is no single definitive way to accomplish this, and numerous charge calculation methods are available in the literature. We chose to calculate the partial atomic charges by using Charge Equilibration (QEq) method[42] available in the LAMMPS[41] package.

The QEq approach in itself is well documented in the literature. However, previous reports of the usage of such methods as applied to simulation of epoxy cross-linking have not provided the full details required to enable reproduction of these charges. For example, the resultant charges can be very sensitive to the values of the taper radius used in the QEq calculations. In the 'Methodological Details' section of the ESI†, we provide complete details of a reproducible process for generating atomic partial charges for both EPON-862, DETDA in isolation (see Figure 2) and for two reacted species; one DETDA with two EPON-862 molecules (Figure 3), and one DETDA with four EPON-862 molecules (see Figure S1 in the ESI†). Herein, we briefly summarize the process.

For the isolated molecules, we modelled EPON-862 we model the 'activated' form of the structure, following Li and Strachan[10]. The activation of EPON-862 was captured by breaking the epoxide bonds (C-O) at both ends of the molecule, with subsequent hydrogenation of these exposed atomic sites. Herein, we denoted the activated form of EPON-862 merely as EPON. We calculated charges for two particular scenarios; 1) for a single (effectively isolated) molecule *in vacuo*, and, 2) for a molecule in the condensed phase. Note that both sets of conditions involved 3-D periodic boundary conditions in the calculation of the charges. We averaged the partial charges for each unique type of atomic environment. The labelling system that illustrates each unique atomic environment is provided in Figure S2 of the ESI†. Since the chemical environment of the atoms in the immediate (and possibly more distant) vicinity of the cross-link bond changes after the cross-link bond is formed, the partial atomic charge distribution for the reacted EPON/DETDA molecule may be different to their counterparts for the unreacted molecules. To account for this, the partial atomic charges after cross-linking were also calculated.

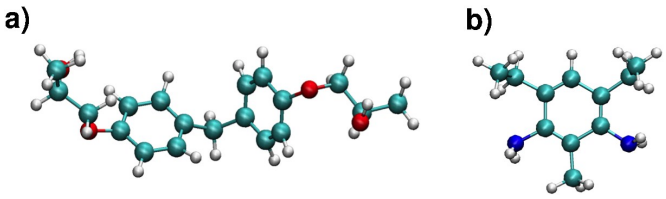

Fig. 2 Molecular structure of a) the activated form of EPON862 molecule and b) the DETDA molecule. Colour code: green, C; blue, N; red, O; white, H).

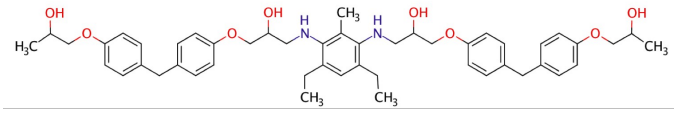

Fig. 3 Product of reaction between two EPON molecules and the primary amine of the DETDA molecule, showing the cross-link bonds.

Pure Liquid EPON and DETDA Modeling

Having established the partial atomic charges, we then proceeded to model the pure liquid phase for both EPON and DETDA. Because the liquid mixture of EPON and DETDA reacts very quickly to form a solid 3-D network, there is no experimental benchmark regarding the density and structure of the liquid mixture against which we could validate our force-field. Therefore, we have used these pure liquid systems as a means to benchmark our simulations and to fine-tune the details of the van der Waals (vdW) interactions (see below). To do this, we prepared two samples; one containing 128 EPON and one containing 128 DETDA molecules. In the ESI† section 'Methodological Details', we provide full details and discussion of the two vdW forms tested in our work; the Lennard-Jones (LJ) and Buckingham (X6) potentials. In particular, the X6 potential can incorporate a dimensionless scaling parameter which may be either kept constant for each atom (denoted here as $X6_{const}$) for all atoms, or can be varied, according to atom type (denoted here as $X6_{var}$)[36].

The pure liquid simulation procedure was as follows. In each case the molecules were randomly packed in a cubic simulation cell using PACKMOL[43]. The initial cubic cell dimensions were $100\times100\times100$ Å^3 and $50\times50\times50$ Å^3 for the pure liquid EPON and DETDA, respectively (such that the initial density of the liquid EPON and DETDA was very low, at 0.3 g cm^{-3} and 0.15 g cm^{-3}, respectively). The structures in these cells were then geometry optimised using the LAMMPS-implemented FIRE algorithm[44], with a maximum of 50000 optimisation steps and limiting the maximum atomic displacement to 0.1 Å to prevent unrealistically large displacements of near-overlapped atoms. After this step, the system temperature was increased up to 1000 K via NVT MD simulation for 50 ps and maintained at this temperature for a further 400 ps, again via NVT MD simulation. Next, the system was lin-

early cooled back to the cross-linking reaction temperature, 500 K (see below), via *NVT* MD simulation for 500 ps. After a further 100 ps NVT MD simulation at 500 K, we used this final structure as input for an *NPT* MD simulation at 500 K and 1 atm for 300 ps. The duration of this *NPT* simulation was found to be sufficient to yield a converged liquid density in each case (see Results section).

Modelling the Liquid Precursor Mixture

From a molecular simulation perspective, care must be taken to ensure the system is well mixed. This is because the structuring of the liquid, if not at equilibrium, could profoundly impact on the resulting 3-D network of cross-linked bonds, and thus lead to misleading predictions. To this end, EPON and DETDA molecules were packed in a cubic simulation cell with the ratio of 2:1 (256:128), using PACKMOL[43]. The initial density of the packed system was deliberately set to a low value, 0.5 g cm^{-3}, which corresponded to the simulation cell length of 70 Å. This was done for the same reason as provided for the pure liquid simulations described earlier. Three samples were independently generated, using initially-random packing of the EPON and DETDA. All subsequent cross-linked sample preparation followed from these three independent samples. System properties, such as the liquid densities, were averaged over these three samples to enhance statistical sampling.

The same geometry optimisation procedure as described for the pure liquids was implemented here. After geometry optimisation, the density of the liquid mixture simulation cell was then calculated using the simulation protocol detailed in the previous section for the pure liquids. Once the density of the liquid mixture at 500 K was established, to ensure adequate mixing we then subjected the liquid mixture to simulated annealling, where the system was heated up and cooled down between 500-1000 K using MD simulation in the *NVT* ensemble to ensure equilibration, using the cell dimensions that resulted from our density calculation. Specifically, each annealing cycle comprised: MD simulation at 500 K, for 0.2 ns; then the temperature was linearly ramped to 1000 K over a period of 0.2 ns, next the system temperature was held at 1000 K for a further 1.0 ns; and finally the system was then cooled back to 500 K over a time period of 0.5 ns.

We calculated several radial distribution functions (RDFs) at 500 K to characterise the internal structure of the liquid mixture. To this end, our reference sites were defined with the center-of-mass (COM) of phenyl ring in the DETDA molecule (denoted CD), and the central carbon atom connected between the two phenyl rings in the EPON molecule (denoted CE). The reference sites on each molecule used to calculate our RDFs are illustrated in Figure S3 of the ESI†. Using in-house developed code, we calculated the CD-CD, CD-CE and CE-CE RDFs and compared these as a function of successive annealing cycles. We saved frames from the trajectory every 1 ps during the first 200 ps of each annealing cycle, and each RDF was averaged over these 200 frames in each cycle. We terminated the simulated annealing process when the difference between RDFs of the successive cycles became negligible; this resulted in a total six annealing cycles in our simulations.

Epoxy Cross-linking Procedure

With our process, we carefully construct a reproducible and reliable 3-D cross-linked epoxy material free from internal stress, from which thermo-mechanical properties of the material can be subsequently predicted via MD simulations. As we shall demonstrate herein, our procedure is an elaboration on the dynamic process. The cross-linking degree in our procedure can be controlled by varying the cross-linking cut-off distance. In our cross-linking procedure we considered the equal probability of primary and secondary amine reactions. As with previously reported studies, the etherification reaction taking place between epoxy and hydroxyl groups, which may compete to epoxy-amine reactions in the presence of excess epoxy groups, was not considered here. Our procedure allows a cross-linked material to be dynamically generated in the presence of external objects, such as surfaces and nanoparticles[45]. To provide a contrast, we also carried out a static cross-linking procedure to highlight the power of our dynamic method. We emphasise here that we do not seek to account for the polymer reaction kinetics in our modelling. The chief purpose of our work is to prepare cross-linked epoxy polymer samples suitable for the subsequent evaluation of their thermo-mechanical properties.

Our cross-linking process is based on a spatial cut-off criterion that is dynamically adjusted during the process. Figure 3 illustrates the reactive atoms in EPON and DETDA molecules that are involved in the cross-link formation. Our initial spatial cutoff between candidate reactive atom pairs (the carbon atom on EPON and the nitrogen atom on DETDA) was set to 3 Å. All potential atom pairs within this distance cut-off in the sample were then linked via a new C–N cross-link bond. The internal stress of the cross-linked polymer increases due to the new bonds created during this stage of the cross-linking process. Therefore, the structure must be relaxed to minimise this internal stress. To accomplish this, we adopted a procedure reported previously Li and Strachan [10], Khare and Khare [17], where we first set the force-constant of the newly-formed cross-linked bonds to be intentionally lower than the actual value, and then gradually increased this force-constant to its target value. At the same time we similarly set the ideal bond length of these newly-formed bonds to be much longer than its actual value, and we concomitantly decreased the ideal bond length to its ideal value, in step with the changes made to the bond force constant.

There were nine stages involved in this relaxation process. At each of the first eight stages, the ideal bond length and the corresponding bond force constant were adjusted to the values indicated in Table S2 in the ESI†, and the system subjected to MD simulation in the *NVT* ensemble for 20 ps, at a temperature of 500 K. At the ninth stage, a 20-ps NPT run at 500 K and 1 atm was carried out. After ten such attempts to locate potential reactive atom pairs for the same given cutoff distance, the system was simulated via NPT MD simulation at 500 K and 1 atm for 50 ps to allow the system to adjust its volume as a response to the formation of new cross-links. Then, the cutoff distance was incremented by 0.5 Å and the steps mentioned above were repeated. Our entire cross-linking procedure was terminated when the de-

gree of cross-linking was achieved. The number of attempts to search for new potential reactive atom pairs was restricted to ten, since we found that after ten cycles, the performance, in terms of number of newly-formed cross-linked bonds *vs.* simulation time, degraded substantially. See Figure 1 for a schematic summary of this cross-linking process. The bonds between the reactive carbon and nitrogen atoms were created using the *fix bond/create* functionality in the LAMMPS simulation package. At the conclusion of our cross-linking procedure, the excess hydrogen atoms connected to all reacted carbon and nitrogen atomic sites and excess bonds (between reacted nitrogen-hydrogen atoms and reacted carbon-hydrogen atoms) were detected via our in-house developed code and deleted by using the *del_bonds* and *del_atoms* commands using LAMMPS. Following this, the system topology along with the distribution of partial atomic charges were updated.

Our cross-linking process was carried out at 500 K which is higher than the typical experimentally reported value[46] of around 450 K. We chose a higher curing temperature because it is well known that the simulated state-point corresponding to a given simulated temperature can be different to the actual state-point. Setting the temperature a little higher than the experimental temperature in our simulations is a conservative measure to ensure the molecules will not become artificially trapped in a glassy state.

To provide a contrast to our approach, we also calculated new bonds via a static method. In the static procedure, all reactive atoms within the reaction distance were detected and the cross-links were formed in one single attempt, starting with a cut-off value of 3 Å. After this point, if the desired degree of cross-linking was not achieved, the cut-off was increased by 0.5 Å until the degree of cross-linking was satisfied. No structural relaxation was performed during the static cross-linking procedure.

Prediction of Thermo-Mechanical Properties

Having obtained three independently-generated cross-linked epoxy polymer samples, we used these to predict a range of thermo-mechanical properties of the material, for comparison with experimentally observed values. Specifically, we report predictions of the glass transition temperature T_g, coefficients of volumetric (α_v) and linear (α_l) expansion, Young's modulus, Poisson's ratio, and the yield stress and yield strain. Our system size for the cross-linked polymer is one of the largest reported for epoxy dynamic cross-linking using all-atom MD simulations (that are not based on dendrimer-like models). Nonetheless, this does not mean that our simulation cell size is sufficiently large to eliminate all size-dependent effects. As reported very recently by Gavrilov *et al.*[24], the simulation cell size can play a role in determining the largest cycle size of the resulting epoxy network topology.

Glass Transition Temperature

The T_g of epoxy resins are strongly dependent on the degree of cross-linking, as well as the thermal history of the sample, such as curing temperature. For example, the same material can have up to $15^{\circ}C$ higher T_g values if the cross-linking reaction has taken place at a higher temperature[47].

In our simulations, we calculated T_g via anisotropic isobaric cooling, where the system was cooled from high to low temperature. Specifically, the system was cooled down from 600 K to 300 K with a cooling rate of 20 K ns^{-1}, via use of MD simulations in the anisotropic *NPT* ensemble, such that the variation in the cell dimensions was fully decoupled in each of the three principal axes. We cooled the system in intervals of 10 K, and simulated the system for 0.5 ns at each temperature point, amounting to a total of 15.5 ns of MD simulation for the cooling of each sample. We calculated the average density of each sample at each temperature point, based on the 500 density values (data-points) calculated from the 0.5 ns trajectory generated at each temperature. Piece-wise data fitting was applied to determine T_g. Two lines were fitted to our resulting temperature *vs.* density curve for the glassy phase and amorphous phase for each sample. The intersection of these two lines is defined as the T_g.

Coefficient of Thermal Expansion

The coefficient of volumetric thermal expansion (CVTE) (α_v) was calculated from the slope of the volume fraction vs. temperature plot, where the volume fraction at a temperature T is $V(T) - V(300)/V(300)$. For isotropic structures, the coefficient of linear thermal expansion (CLTE) (α_l) is simply one-third of the coefficient of volumetric thermal expansion (CVTE). α_v and α_l were calculated by following Eqn. 1.

$$\alpha_v = \frac{1}{V_0}(\frac{\partial V}{\partial T})_P \quad and \quad \alpha_l = \frac{\alpha_v}{3} \tag{1}$$

α_v can be calculated during the isobaric cooling of the material and by recording the volume data at each temperature (following the same cooling simulation procedure as outlined for our T_g calculation). From the slope of volume fraction *vs.* temperature plot we can calculate α_v for both glassy and rubbery states. As was the case for our T_g simulations, we fitted two lines to these data, one each for the glassy and rubbery states.

Stress-Strain Curve

The stress-strain curve (SSC) indicates the spatial deformations of a material when a stress is applied. In our simulations, Young's modulus was obtained from the slope of SSC. Only the linear portion of the SSC, up to 4% strain was used. Littell *et al.*[48] showed that the value of Young's modulus can increase with the increase in strain rate. Therefore, the value of Young's modulus predicted via MD simulations is expected to result in higher values due to fact that MD simulations by necessity must make use of remarkably higher strain rates than those used in experiment. In addition, Poisson's ratio was calculated by plotting the strain in the direction where stress is applied *vs.* the average strain of the other two directions.

Epoxy polymers show brittle behaviour under applied stress. Unlike ductile materials, it is not easy to determine the yield point of brittle materials, where the transition from elastic to plastic behaviour as a response to the applied stress, occurs. The yield point is the point that marks the onset of plastic deformation. Since the yield point is not well-defined in brittle materials, we make use of the 0.2% offset line to find the yield point, which is the conventional treatment in experimental studies (for example, see

Hockney *et al.* [49]). In this convention, a line parallel to the linear part of the SSC curve, shifted by 0.2% is drawn and the intersection point with the SSC is determined, which is by definition identified as the yield point. The yield stress and strain are found as projections in strain and stress axes, as illustrated in Figure S4 of the ESI†.

Here we performed a tensile test, where the epoxy polymer was deformed under tension with a constant strain rate. The mechanical properties of a material can be calculated *via* non-equilibrium MD methods. The *fix deform* command of LAMMPS was used for our constant strain simulations. Constant strain was applied to each principal axis of the simulation cell in different simulations, while the cell dimensions in the other two directions was free to change. Atmospheric pressure (1 atm) was applied to the other two cell dimensions so as to enable them to independently respond dynamically to the applied stress. Our applied strain rate was 5×10^7 s^{-1}. The kinetic response of atoms to the applied strain was accounted for by using MD simulations in the *NPT* ensemble using anisotropic coupling, at a constant temperature of 300 K. For each principal direction in each sample, we modelled the response to the applied stress ranging from 0% to 20% strain, over a simulation duration of 4 ns (using 4000 stress-strain data points per run to construct the SSC). This amounted to nine SSC simulations overall with a total of 36 ns of MD simulation.

In an experimental setting, the cross-sectional area of a specimen may change as the deformation occurs. Within the definitions of the engineering SSC, the cross sectional area of the specimen is considered as constant. However, within the definitions of the true SSC, the cross-sectional area may change as a function of applied stress. The engineering SSC was calculated via non-equilibrium MD simulations, while the true SSC was calculated by using the engineering stress-strain data *via* Eqn. 2:

$$\sigma = s(1+e) \text{ and } \varepsilon = ln(1+e) \quad (2)$$

where s and e are the engineering stress and strain, and σ and ε are the true stress and strain, respectively.

Results and Discussion

Partial Charge Calculations

For the unreacted EPON and DETDA molecules, we calculated the partial atomic charges over all atomic sites of each molecule using both the 'vacuum' and 'condensed phase' models. Figure 4 shows the calculated partial charges by the use of the vacuum model (calculated over one single molecule) and condensed phase model (a system including 16 EPON and 8 DETDA molecules) for both EPON and DETDA molecules. The full set of partial atomic charges as calculated by the 'vacuum' configuration are provided in Table S3 of the ESI†. Although the study reported by Li and Strachan [10] indicated that the charges calculated in vacuum and condensed phase were different, our results revealed no remarkable difference in the partial atomic charges calculated via both procedures; as reported in Figure 4. However, due to the lack of key details in the study of Li and Strachan [10], we cannot comment further on this discrepancy. Based on this evidence, herein, we have used the 'vacuum' environment for the calculation of our partial charges.

In addition, we calculated the partial atomic charges of the reacted EPON and DETDA systems (see Methods) and compared this set of partial atomic charges with those calculated for the unreacted molecules. In Figure 5 we plot the partial atomic charges of EPON and DETDA before *vs.* after the cross-linking reaction for both the primary and secondary amine reactions. Figure 5 reveals that the only atomic sites that show significant deviation from the unreacted partial charges are chiefly the atoms participating the reaction, *i.e.* the carbon atom of EPON and the nitrogen atom of DETDA. This was found to be the case for both the primary and secondary amine reactions. Based on this evidence, we decided to only update the charges of the two reacted (carbon and nitrogen) atoms upon cross-linking. Table 1 provides the new partial atomic charges of the reacted carbon atom of the EPON molecule and the nitrogen atom of the DETDA molecule for the primary and secondary reactions.

Table 1 Partial atomic charges of the reacted carbon and nitrogen atoms of EPON and DETDA, respectively, for the primary and secondary amine reactions.

Atom	Charge / esu		
	Unreacted	Primary	Secondary
C	-0.3576	-0.18195	-0.1927
N	-0.7496	-0.51765	-0.2642

Density of Pure Liquids: EPON and DETDA

As part of the process to check the DREIDING force-field (including our calculated partial atomic charges), the density values of pure liquid EPON and DETDA were calculated at 300 K and 1 atm from our MD simulations in the *NPT* ensemble (see Methods) and compared with experimental values, employing a three variations on the description of the van der Waals interaction. Using the X6$_{\text{const.}}$ form of the Buckingham potential (see Methods), the density values for pure liquid EPON and pure liquid DETDA at 300 K and 1 atm were predicted to be 1.132 ± 0.005 g cm^{-3} and 0.982 ± 0.007 g cm^{-3}, respectively. The corresponding experimental values are 1.174 g cm^{-3} for EPON [50] at 298 K, and 1.022 g cm^{-3} for DETDA [51] at 293 K. We also tested the performance of the X6$_{\text{var.}}$ form of the Buckingham potential in predicting these liquid densities, as well as the Lennard-Jones (LJ) form of this interaction. Our results yielded markedly lower densities for both pure liquids compared with those supported by the X6$_{\text{const.}}$ form of the Buckingham potential and the corresponding experimental values. Plots of liquid density *vs.* simulation time, indicating the equilibration of the density, are shown for all cases in Figure S5 of the ESI†. These data indicate that the X6$_{\text{const.}}$ form of the Buckingham potential should yield best performance for modelling the liquid precursor mixture.

Density and Structure of the EPON/DETDA Liquid Mixture

Because of the rapid reaction between the two precursors, there are no experimental data available regarding the density and structure of the liquid mixture of EPON and DETDA. In this in-

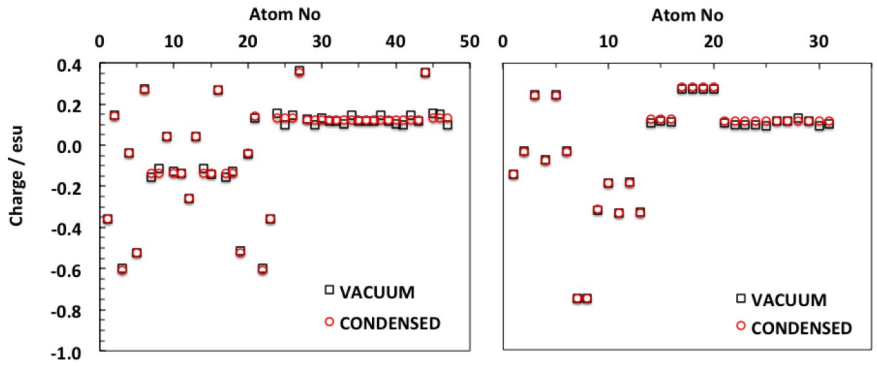

Fig. 4 Partial atomic charges (a) for EPON (b) DETDA calculated for both the 'isolated' (vacuum) and 'condensed phase' environments.

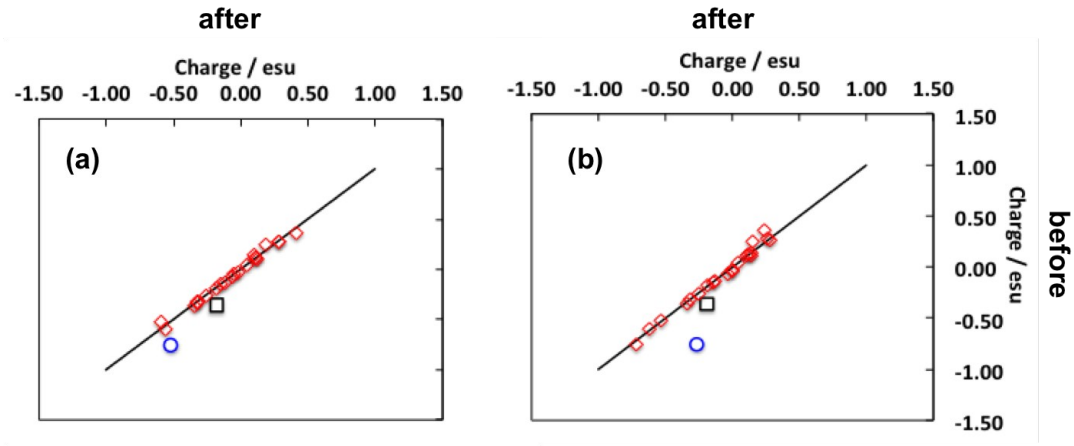

Fig. 5 Partial atomic charges of EPON and DETDA before and after cross-linking (blue circle for reacted N, black square for reacted C) **(a)** primary amine reaction, **(b)** secondary amine reaction.

stance, as a check to ensure our predictions of liquid density were sensible, we used existing experimental data taken from the pure liquid systems[50,51] to infer the density of the ideal EPON/DETDA liquid (with a EPON/DETDA ratio of 2:1), based on the ideal mixing law. This yielded an estimated ideal density of 1.137 g cm^{-3}. The corresponding value at 300 K, predicted from our MD simulations in the *NPT* ensemble using the X6$_{\text{const.}}$ form of the Buckingham potential was 1.101±0.003 g cm^{-3}. While the comparison with our inferred experimental value is not expected to yield perfect agreement, our results indicate that our predictions are reasonable. Because we carried out the cross-linking procedure at 500 K (see Methods), we also predicted the density of the liquid precursor mixture at this temperature. The density was averaged over our three independent samples to yield 0.988±0.005 g cm^{-3} at 500 K. The evolution of the system density with time is shown in Figure S6 of the ESI† for various cases. In Figure S6c) of the ESI† we provide the time evolution of the density at 500 K with respect to simulation time for all three samples, showing the close agreement of each final density.

We also tested the influence of the partial atomic charges on the packing of molecules in the liquid mixture. This was evaluated by switching off the Coulombic interactions in our 500 K MD simulations, with equilibration of the density performed as described earlier. A comparison of the densities from the "no-charges" system and from the regular system is also reported in Figure S6d) of the ESI†. The presence of the Coulombic interactions had a beneficial effect on the packing of the molecules, yielding a higher density compared with the "no-charges" case. Based on our evidence for both the pure liquids and the liquid mixture, we used X6$_{\text{const.}}$ parameters for all other simulations reported herein.

After identifying which form of the vdW interaction to use, we then predicted the structuring of the liquid mixture at our curing temperature of 500 K and 1 atm. We accomplished this by calculating radial distribution functions (RDFs) for EPON-EPON (CE-CE), DETDA-DETDA (CD-CD) and EPON-DETDA (CE-CD) contacts from our simulated annealing MD simulations, as summarized in the Methods. Evidence of the equilibration of the structuring of the liquid mixture, indicated by the evolution of the three RDFs as a function of simulated annealing cycle, for each of our three samples, is presented in Figure S7 of the ESI† The resulting RDFs generated after six simulated annealling cycles are shown in Figure 6. The first peak in the CE-CE distribution was located at 5.4 Å while the first peak corresponding with the CD-CE distribution is found at a greater separation, since the CD site is

not a single atom, but rather the centre-of-mass of the six phenyl carbon atoms in DETDA. This may also explain why the CD-CD RDF appears relatively noisier. The first peak in the CD-CD RDF was found at 4.9 Å. Based on the visualisation of the structure, we observed that the phenyl rings of DETDA molecules were arranged in a slipped parallel alignment, with a significant lateral shift between the phenyl rings, which may account for the shoulder at 4.9 Å.

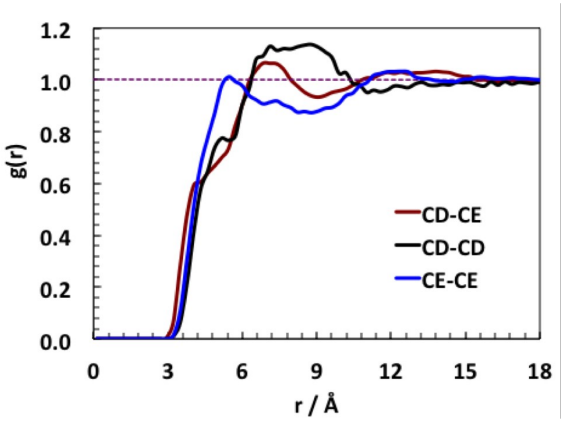

Fig. 6 RDFs of the liquid precursor mixture calculated between (a) CD-CE, (b) CE-CE, and (c) CD-CD, generated from simulations at 500 K and 1 atm.

Epoxy Cross-linking Procedure and Sample Relaxation

Once we had established that our three liquid precursor mixture samples were structurally equilibrated, we applied our in-situ cross-linking procedure to these samples. For comparison, we also carried out a static cross-linking process (see Methods). Figure 7 shows the variation in the degree of cross-linking in our samples as a function of the cut-off distance between candidate reactive atoms (see Methods), as generated for both our process and the static process. As is clearly seen from Figure 7, the our cross-linking procedure yielded a higher degree of cross-linking when compared to the static process for a given cut-off distance. All three samples yielded a similar profile of cross-linking degree *vs.* cut-off distance which is clear evidence of well-mixed and equilibrated liquid precursor mixture samples. Since more reactive atom pairs are available at the beginning of the process, the rate at which new cross-links are generated slows as the degree of cross-linking increases, as indicated in Figure 7. After each attempt to form cross-links, we extensively relaxed the structure via *NVT* and *NPT* MD simulations to allow the molecules to diffuse during this relaxation. We deliberately used a long, step-wise procedure not just for the relaxation of the resultant structure, but also to allow the molecules to diffuse so as to bring remaining reactive atoms closer to each other for the next cross-linking attempt. The data in Figure 7 show that for a given cut-off distance, these relaxation steps do indeed result in an increase in cross-link formation, which can only arise due to diffusion of molecules in the sample. This increase clearly diminishes as the degree of cross-linking approaches ∼90% (*e.g.* corresponding to a cut-off of 7 Å). The cross-linked epoxy polymer structures used in our subsequent thermo-mechanical property simulations all had a degree of cross-linking of 78%, which was obtained at a maximum cut-off distance of 4.5 Å in our procedure.

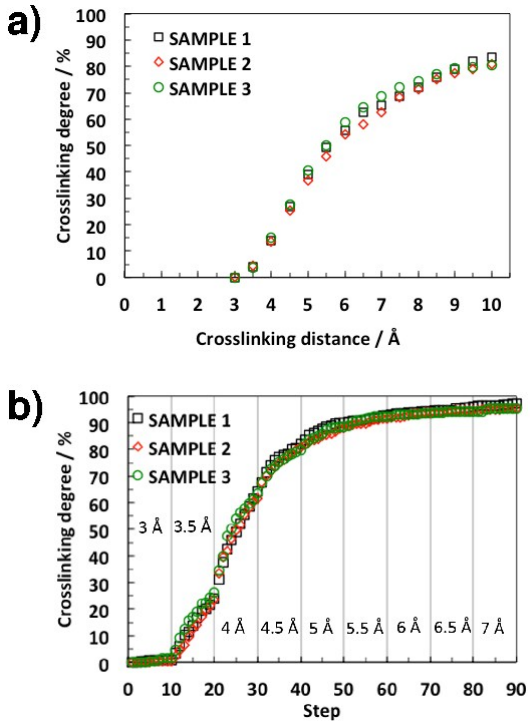

Fig. 7 Variation in the degree of epoxy cross-linking as a function of cut-off distance for both (a) static procedure, and (b) our dynamic procedure.

At the end of the cross-linking procedure (when the degree of cross-linking reached 78%), the bond lengths between the reacted epoxide carbon and amine nitrogen atoms were measured and compared with the equilibrium bond length as defined by the DREIDING FF[36]. A similar analysis was carried out for the related C-N-C angles. Figure S8a) in the ESI† shows these bond length and angle distributions obtained from the trajectories after the cross-linking. The calculated average cross-link bond lengths and associated bond angles at 500 K were 1.490±0.002 Å and 112.302±0.760°, while the corresponding ideal values in the DREIDING FF are 1.462 Å and 109.471°, respectively. The dashed lines in Figure S8 in the ESI† correspond with these ideal bond length and angle values. The differences between calculated and ideal values may be ascribed to the high temperature of the system (500 K).

In addition, the internal pressure of the resulting cross-linked samples was checked to verify whether each sample was internally stress-free. Figure S9 in the ESI† shows the pressure distributions obtained via our *NPT* MD simulations after the termination of the cross-linking process (see Methods). Our results show that the total pressure of the sample fluctuated around 1 atm pressure (indicated by the dashed line in Figure S9 in the ESI†). Fluctuations of pressure of this magnitude are entirely typical for an equilibrated *NPT* MD simulation[52].

Prediction of Polymer Thermo-Mechanical Properties

We used our three independently-generated cross-linked polymer samples, each with a cross-linking degree of 78%, to calculate thermo-mechanical properties of the epoxy. T_g, α_v, and α_l were predicted via the analysis of our isobaric cooling simulations (see Methods). Young's Modulus, Poisson's ratio, and the yield strain and stress were calculated via non-equilibrium MD simulations.

As described in the Methods, each of our three cross-linked structures was first simulated at 600 K and cooled down from this temperature to 300 K. The density value averaged over the three samples at 300 K 1.180±0.001 g cm^{-3}, which is in good agreement with the experimental value[53] of around 1.200 g cm^{-3}.

In the literature, the experimentally measured T_g range for the system under consideration is 108.0–161.1 K[46,47,54–58]. However, T_g is a function of the cross-linking degree, which may account for the wide range of T_g values reported in the literature. The discrepancy between values might also be attributed to differences in the curing schedule. Figure 8a) shows the predicted polymer density, ρ, as a function of temperature, calculated as an average over our three samples.

Because our cooling rate in the MD simulations was much greater than the experimental cooling rates, our predicted T_g values are expected to be an over-estimate of the experimentally-determined values. To reflect this mismatch between the experimental and computational cooling rates, a commonly-applied correction is to add approximately 3 K per order of magnitude in the cooling rate to the experimental T_g value[59], for the purposes of fair comparison with the simulation-based T_g value. Alternatively, this correction can be subtracted off the simulation-based estimate of T_g. In our case, Rangari *et al.*[57] carried out their experimental thermal analysis at a cooling rate of 10 °C min^{-1}, which was approximately 11 orders of magnitude lower than our cooling rate (1.2 ×10^{12} °C min^{-1}). Therefore, our adjusted simulation-based T_g value reduced to 407-417 K (134-144 °C).

Figure 8b) shows the dependence of polymer volume fraction with system temperature, from which α_v (the coefficient of volumetric thermal expansion) was calculated as an average over our three cross-linked samples. This yielded α_v values of 424.3×10^{-6} K^{-1} and 258.2×10^{-6}K^{-1} for the glassy and rubbery states respectively. This resulted in α_l values of 141.4×10^{-6} K^{-1} and 86.1×10^{-6} K^{-1} for the glassy and rubbery states, respectively. The corresponding experimentally-reported α_l values[55] are 180×10^{-6}K^{-1} and 64×10^{-6}K^{-1} for glassy and rubbery states, respectively. We again note that, as is the case for other thermo-mechanical properties, the CTE values are function of the cross-linking degree of the polymer.

Stress-Strain Response

Figure 9a) shows both the engineering and true stress-strain (SSC) curves of the polymer calculated as the average over our three samples, each with a 78% degree of cross-linking. As expected, the engineering SSC deviates from the linearity as lower strain values compared with the true SSC. We obtained Young's modulus values from the SSCs up to 4% strain, as shown in Figure 9a) (see also Figure S10 of the ESI†). The sample-averaged Young's modulus values were 2.85 and 3.02 GPa calculated from

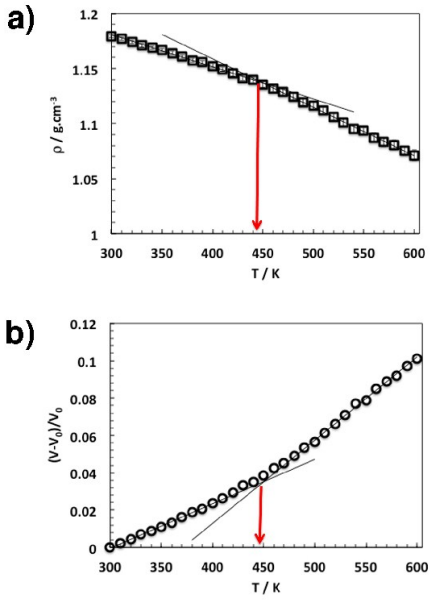

Fig. 8 Predicted thermal properties of the epoxy polymer with a 78% cross-linking degree. a) System density as a function of temperature, and b) volume fraction as a function of temperature.

engineering and true SSCs, respectively. The experimentally reported Young's modulus values varied between 2.52 and 2.89 GPa as reported by Littell *et al.*[48] and 2.7 and 3.25 GPa[58]. We can ascribe the discrepancy between our predicted results and the experimental values to two key factors. First, the higher strain rate inherent to the MD simulations leads to higher Young's modulus values. Second, we do not know the cross-linking degrees of the samples used in the experimental studies, which limits direct comparisons because Young's modulus of epoxy polymer is highly dependent on the cross-linking degree.

In Figure 9b) we show the strain-strain data used to obtain Poisson's ratio from the engineering and true SSCs. The average values were 0.38 and 0.39 calculated from the engineering and true SSCs, respectively. The experimentally calculated Poisson's ratios varied between 0.40 and 0.43[48]; again, the caveat regarding the dependence on the degree of cross-linking applies here.

The yield strength and yield strain were calculated from the engineering and true SSCs, as provided in Figure S11 of the ESI†. The solid lines represent the 0.2% offset lines which were used to determine the yield points. It should be noted here that the force-field used in this study is not able to capture bond breakage. Therefore, the maximum value obtained in the SSCs may not be truly representative of the breakage point, because the material could be broken before the maximum point in the predicted SSCs. Therefore, it is more appropriate to focus on the yield point where the first plastic deformations take place.

As it is seen clearly from Figure S11 of the ESI†, the 0.2% offset line intersected the SSCs at 4.2% strain. Since the epoxy polymer samples show no or modest plastic deformation, we can expect that the breakage takes place at around this range. Littell *et al.*[48] reported a failure strain of 4.02% strain for this material, while Sun *et al.*[56] reported a lower value for the failure elongation,

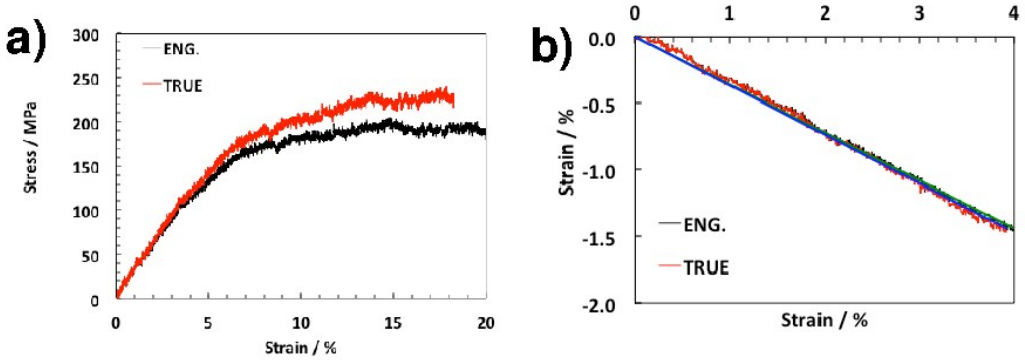

Fig. 9 Predicted mechanical properties of the epoxy polymer with a 78% cross-linking degree. a) Average engineering and true stress-strain curves, and b) strain-strain curve for calculation of Poisson's ratio.

of 3.24% strain, just before fracture. The differences may be attributed to the cross-linking degree of the specimens as well as the process history of the specimens used in these experimental studies. In addition, our calculated yield strength was in the range of 110 – 120 MPa; however, there are no experimental data available regarding the yield stress for these epoxies in the literature.

Conclusions

In summary, we have introduced a comprehensive, robust and reproducible molecular simulation protocol for the generation and property evaluation of epoxy polymer samples. Our protocol has been reported in sufficient detail to allow full reproduction of our results at each step, it can be extended to any general thermoset polymer, it is amenable for use with a wide range of force-fields, and has been devised for implementation with freely-available software. Key to our protocol was the inclusion of a reproducible procedure for calculation of partial atomic charges; a reliable process for equilibration of the liquid precursor mixture; a robust protocol for generating the three-dimensional cross-linked polymer; and the use of independently-generated samples, starting at the point of the liquid precursor mixture. While helpful for studying pure polymer systems, our dynamic cross-linking procedure will also be valuable in the preparation of polymer samples that are dynamically cross-linked in the presence of surfaces and nanostructures, which will allow the details of the interphase associated with these interfacial systems to be captured.

Acknowledgments

We gratefully acknowledge funding from the ARC DP130100404. We thank the NCI for access to computing facilities via the Deakin University collaboration agreement. B.D. thanks CSIRO and Deakin for an AFFRIC PhD scholarship. T.R.W. thanks **veski** for research funding and for an Innovation Fellowship.

References

1 Y. Zhou, F. Pervin, L. Lewis and S. Jeelani, *Mat. Sci. Eng. A-Struct.*, 2007, **452–453**, 657 – 664.
2 I. S. Klaus and W. S. Knowles, *J. Appl. Polym. Sci.*, 1966, **10**, 887–889.
3 I. Yarovsky and E. Evans, *Polymer*, 2002, **43**, 963 – 969.
4 J. Gou, B. Minaie, B. Wang, Z. Liang and C. Zhang, *Comp. Mater. Sci.*, 2004, **31**, 225 – 236.
5 D. R. Heine, G. S. Grest, C. D. Lorenz, M. Tsige and M. J. Stevens, *Macromolecules*, 2004, **37**, 3857–3864.
6 C. Wu and W. Xu, *Polymer*, 2006, **47**, 6004 – 6009.
7 P. V. Komarov, C. Yu-Tsung, C. Shih-Ming, P. G. Khalatur, and P. Reineker, *Macromolecules*, 2007, **40**, 8104–8113.
8 H. B. Fan and M. M. Yuen, *Polymer*, 2007, **48**, 2174 – 2178.
9 V. Varshney, S. S. Patnaik, A. K. Roy and B. L. Farmer, *Macromolecules*, 2008, **41**, 6837–6842.
10 C. Li and A. Strachan, *Polymer*, 2010, **51**, 6058 – 6070.
11 H. Hörstermann, R. Hentschke, M. Amkreutz, M. Hoffmann and M. Wirts-Rütters, *J. Phys. Chem. B*, 2010, **114**, 17013–17024.
12 N. Nouri and S. Ziaei-Rad, *Macromolecules*, 2011, **44**, 5481–5489.
13 A. Bandyopadhyay, P. K. Valavala, T. C. Clancy, K. E. Wise and G. M. Odegard, *Polymer*, 2011, **52**, 2445 – 2452.
14 N. B. Shenogina, M. Tsige, S. S. Patnaik and S. M. Mukhopadhyay, *Macromolecules*, 2012, **45**, 5307–5315.
15 A. Bandyopadhyay and G. M. Odegard, *Modelling Simul. Mater. Sci. Eng.*, 2012, **20**, 045018.
16 A. Izumi, T. Nakao and M. Shibayama, *Soft Matter*, 2012, **8**, 5283–5292.
17 K. S. Khare and R. Khare, *Macromol. Theor. Simul.*, 2012, **21**, 322–327.
18 T. Okabe, T. Takehara, K. Inose, N. Hirano, M. Nishikawa and T. Uehara, *Polymer*, 2013, **54**, 4660 – 4668.
19 G. M. Odegard, B. D. Jensen, S. Gowtham, J. Wu, J. He and Z. Zhang, *Chem. Phys. Lett.*, 2014, **591**, 175 – 178.
20 D. R. Xin and Q. Han, *J. Mol. Model.*, 2015, **21**, year.
21 C. Li, E. Coons and A. Strachan, *Acta Mech.*, 2014, **225**, 1187–1196.
22 I. Hamerton, W. Tang, J. V. Anguita and S. R. P. Silva, *React. Funct. Polym.*, 2014, **74**, 1–15.
23 J. D. Monk, J. B. Haskins, C. W. B. Jr. and J. W. Lawson, *Polymer*, 2015, **62**, 39–49.
24 A. A. Gavrilov, P. V. Komarov and P. G. Khalatur, *Macro-*

molecules, 2015, **48**, 206–212.
25 C. Jang, T. W. Sirk, J. W. Andzelm and C. F. Abrams, *Macromol. Theor. Simul.*, 2015, **24**, 260–270.
26 C. A. Krausse, T. Milek and D. Zahn, *J. Mol. Model.*, 2015, **21**, 263.
27 C. Li and A. Strachan, *J. Polym. Sci. Pol. Phys.*, 2015, **53**, 103–122.
28 J. L. Tack and D. M. Ford, *J. Mol. Graph. Model.*, 2008, **26**, 1269 – 1275.
29 W. L. Jorgensen, D. S. Maxwell and J. Tirado-Rives, *J. Am. Chem. Soc.*, 1996, **118**, 11225–11236.
30 A. C. T. van Duin, S. Dasgupta, F. Lorant and W. A. Goddard, *J. Phys. Chem. A*, 2001, **105**, 9396–9409.
31 S. Masoumi, B. Arab and H. Valipour, *Polymer*, 2015, **70**, 351 – 360.
32 C. Li and A. Strachan, *Polymer*, 2011, **52**, 2920 – 2928.
33 C. Li, A. R. Browning, S. Christensen and A. Strachan, *Compos. Part A-Appl. S.*, 2012, **43**, 1293 – 1300.
34 C. Li, G. A. Medvedev, E.-W. Lee, J. Kim, J. M. Caruthers and A. Strachan, *Polymer*, 2012, **53**, 4222 – 4230.
35 C. Li, E. Jaramillo and A. Strachan, *Polymer*, 2013, **54**, 881 – 890.
36 S. L. Mayo, B. D. Olafson and W. A. Goddard, *J. Phys. Chem*, 1990, **94**, 8897–8909.
37 S. Nosé, *J. Chem. Phys.*, 1984, **81**, 511–519.
38 W. G. Hoover, *Phys. Rev. A*, 1985, **31**, 1695.
39 W. G. Hoover, *Phys. Rev. A*, 1986, **34**, 2499.
40 R. Hockney and J. Eastwood, *Computer Simulation Using Particles*, Taylor & Francis Group, 1988.
41 S. Plimpton, *J. Comp. Phys.*, 1995, **117**, 1–19.
42 A. K. Rappe and W. A. Goddard, *J. Phys. Chem.*, 1991, **95**, 3358–3363.
43 L. Martínez, R. Andrade, E. G. Birgin and J. M. Martínez, *J. Comput. Chem.*, 2009, **30**, 2157–2164.
44 E. Bitzek, P. Koskinen, F. Gähler, M. Moseler and P. Gumbsch, *Phys. Rev. Lett.*, 2006, **97**, 170201.
45 S. J. Tucker, B. Fu, S. Kar, S. Heinz and J. S. Wiggins, *Compos. Part A.-Appl. S.*, 2010, **41**, 1441–1446.
46 S. G. Miller, G. D. Roberts, C. C. Copa, J. L. Bail, L. W. Kohlman and W. K. Binienda, *Effects of Hygrothermal Cycling on the Chemical, Thermal, and Mechanical Properties of 862/W Epoxy Resin*, Nasa 2011-216999, 2011.
47 K. Tao, S. Yang, J. C. Grunlan, Y.-S. Kim, B. Dang, Y. Deng, R. L. Thomas, B. L. Wilson and X. Wei, *J. Appl. Polym. Sci.*, 2006, **102**, 5248–5254.
48 J. Littell, C. Ruggeri, R. Goldberg, G. Roberts, W. Arnold and W. Binienda, *J. Aerospace Eng.*, 2008, **21**, 162–173.
49 R. W. Hockney, J. W. Eastwood, J. Schwiedrzik, R. Raghavan, A. Bürki, V. LeNader, U. Wolfram, J. Michler and P. Zysset, *Nat. Mater.*, 2014, **13**, 1476–1122.
50 http://www.momentivespecialtychemicals.com/Products/TechnicalDataSheet.aspx?id=3950.
51 http://www.lonza.com/products-services/industrial-solutions/high-performance-materials/lonzacure-hardeners/lonzacure-detda-80.aspx.
52 R. Rahman and A. Haque, *Compos. Part. B-Eng.*, 2013, **54**, 353 – 364.
53 http://www.evroberts.com/EVRTDS/49/EPIKOTE.
54 Z. Wang, Z. Liang, B. Wang, C. Zhang and L. Kramer, *Compos. Part A.-Appl. S.*, 2004, **35**, 1225 – 1232.
55 S. Wang, Z. Liang, P. Gonnet, Y.-H. Liao, B. Wang and C. Zhang, *Adv. Funct. Mater.*, 2007, **17**, 87–92.
56 L. Sun, G. Warren, J. O'Reilly, W. Everett, S. Lee, D. Davis, D. Lagoudas and H.-J. Sue, *Carbon*, 2008, **46**, 320 – 328.
57 V. Rangari, M. Bhuyan and S. Jeelani, *Compos. Part A.-Appl. S.*, 2011, **42**, 849 – 858.
58 2015, http://www.evroberts.com/EVRTDS/49/EPIKOTE.
59 M. L. Williams, R. F. Landel and J. D. Ferry, *J. Am. Chem. Soc.*, 1955, **77**, 3701–3707.

Graphical Abstract for: A robust and reproducible procedure for cross-linking thermoset polymers using molecular simulation

Baris Demir[a] **and Tiffany R. Walsh**[*a]

a Institute for Frontier Materials, Deakin University, Geelong, 3216, VIC, Australia; tiffany.walsh@deakin.edu.au

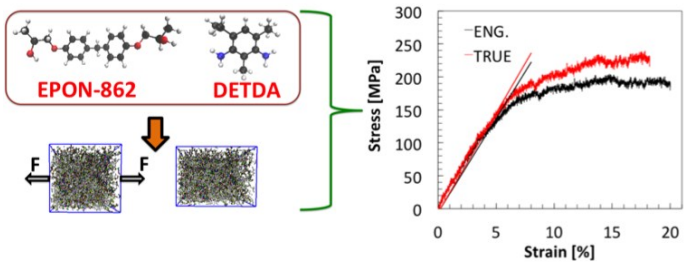

Our reliabile and reproducible cross-linking procedure ranges from careful equilibration of the liquid polymer precursor to calculating the thermo-mechanical properties of the cross-linked polymer. Our appoach can be used to cure not only pure thermoset polymers, but also thermoset-based composite materials.